THE JOURNAL OF PHYSICAL CHEMISTRY C

Article

pubs.acs.org/JPCC

Screening of Copper Open Metal Site MOFs for Olefin/Paraffin Separations Using DFT-Derived Force Fields

Ambarish R. Kulkarni[†] and David S. Sholl*[,‡]

[†]Department of Chemical Engineering, Stanford University, Stanford, California 94305, United States

[‡]School of Chemical and Biomolecular Engineering, Georgia Institute of Technology, Atlanta, Georgia 30332, United States

Supporting Information

ABSTRACT: Efficient processes for adsorptive separation of light olefin/paraffin mixtures are likely to have many advantages over traditional separation techniques for these commodity chemicals. Although some metal organic frameworks (MOFs) have been studied experimentally for this process, a large-scale computational screening study has not been reported due to the inherent difficulty in describing the critical role of interactions of olefins with open metal sites (OMS). In this paper, we introduce new density functional theory (DFT) derived force fields (FFs) that accurately describe adsorption of C_2 and C_3 olefins and paraffins in CuBTC. Using detailed DFT calculations for MOF-505 and PCN-16, we show that the energetics predicted by our FFs are transferable to other related MOFs that contain Cu OMS. Next, we evaluate the performance of 94 distinct Cu−OMS MOFs for the industrially important propylene/propane separation and identify 18 MOFs predicted to have attractive properties as adsorbents. Finally, we show that the ideal adsorbed solution theory is inaccurate for inhomogeneous olefin/MOF systems and present extensive binary propane/propylene adsorption isotherms for the top-performing MOFs identified in our calculations.

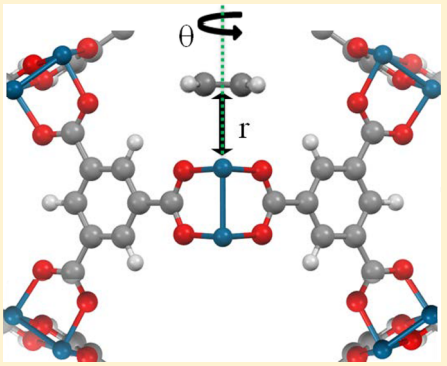

Downloaded via UNIV OF CALIFORNIA DAVIS on August 9, 2021 at 20:53:33 (UTC).
See https://pubs.acs.org/sharingguidelines for options on how to legitimately share published articles.

1. INTRODUCTION

Owing to an increased availability of hydrocarbon gas liquids (HDL)[1] and completion of new processing facilities, ethylene and propylene capacities are estimated to reach 1.6 million barrels per day (bbl/d) and 600000 bbl/d by 2018, respectively.[2] In production of these bulk chemicals, a catalytic cracking process is followed by high-pressure cryogenic distillation of the olefin/paraffin mixtures, which results in a severe energy penalty (>10^{14} BTU/yr).[3−6] Given the huge scale of production, alternate energy-efficient processes for separation of light hydrocarbons will result in lower costs and reduced CO_2 emissions. One such promising strategy is the selective separation of olefins by nanoporous adsorbents such as metal organic frameworks (MOFs).[4,7]

Considerable interest has been focused on using MOFs as adsorbents for olefin/paraffin separations.[3,4,8−10] A strategy that has attracted special attention is using MOFs with coordinatively unsaturated metal sites where the π-double-bond interactions between olefins and open metal sites lead to preferential interactions relative to paraffins.[3,11,12] One reason for the growing popularity of MOFs is the diversity of materials that have been synthesized.[13,14] However, due to the huge number of structures and possible chemical modifications, detailed experiments involving a large subset of materials are impractical.

This has led to multiple efforts using computational screening to identify materials with useful performance for different chemical separations.[15−24] For computational screening of MOFs as potential adsorbents to be effective, force fields (FFs) that accurately capture the interactions between adsorbed molecules and MOFs must be available. Although generic FFs can give a reasonable description of physisorption of simple species such as H_2[25,26] and CH_4,[27,28] these FFs fail to correctly describe interactions of CO_2,[29−33] H_2O,[34,35] and olefins[11] with open metal sites (OMS) in MOFs. Previously, FFs based on ab initio calculations have been developed for describing H_2O and CO_2 adsorption in HKUST-1 and MOF-74, two prototypical materials with open metal sites.[17,35−37]

In this paper, we introduce new ab initio FFs that accurately describe adsorption of C_2 and C_3 olefins and paraffins in MOFs containing open Cu sites. These FFs are developed using extensive electronic structure calculations for the adsorption energies of molecules in CuBTC, and the validity of the FFs is examined by comparing predicted adsorption isotherms from the FFs with available experimental data. We also show, by further comparisons with data from electronic structure calculations, that our new FFs are transferable to other MOFs containing open Cu sites. This is an important step because it opens the possibility of using our FFs to predictively investigate olefin/paraffin separations in a wide range of materials. To that end, we evaluate the performance of 94 distinct MOFs that contain copper open metal sites for propylene/propane separations. We find that the simple ideal adsorbed solution theory (IAST) is no longer applicable for

Received: July 26, 2016
Revised: September 16, 2016
Published: September 19, 2016

© 2016 American Chemical Society

DOI: 10.1021/acs.jpcc.6b07493
J. Phys. Chem. C 2016, 120, 23044−23054

inhomogeneous olefin/MOF system. This approach identifies multiple materials that are predicted to have attractive properties as adsorbents for this industrially important process.

2. COMPUTATIONAL DETAILS

Given the availability of consistent experimental hydrocarbon adsorption data from multiple groups, we first focus on CuBTC for developing our FF.[12,38−40] Several previous studies have made empirical corrections to generic FFs in an effort to predict hydrocarbon adsorption in CuBTC.[41−43] Although this approach can improve the fit to measured experimental data, it is unreasonable to expect that these approaches can correctly describe the nature of the relevant olefin−OMS interaction. Moreover, due to differences in the MOF synthesis, activation, and isotherm measurement protocols, the transferability of these experimentally fitted FFs to other MOFs is limited.[44] A notable exception is the work by Fischer et al.,[11,40,45] who used cluster DFT calculations (using the PBE functional) to develop a FF for ethylene and propylene in CuBTC. This FF showed good agreement with experimental olefin isotherms at various temperatures, but the transferability of this FF to other related materials was not explored.[12]

To improve the ease of transferability of our FF to other MOFs, we assume that the nonmetal linker atoms (C, O, and H) in the CuBTC framework are described by the generic DREIDING FF.[46] We acknowledge that this is a strong assumption, and we test its validity below by comparison with reliable experimental adsorption data for CuBTC and with electronic structure calculations in several other Cu-based MOFs. The united-atom (UA) TraPPE FF accurately describes hydrocarbon fluid phase properties and is used for the hydrocarbon atoms.[47] As the UA TraPPE description of alkanes and alkenes does not include point charges or other electrostatic interactions, we do not consider any Coulombic interactions in our hydrocarbon FF. Similar to previous screening studies, the MOF framework is assumed to be rigid during adsorption simulations.[17,37]

Taking the approach outlined above, the key step in developing a FF that describes interactions in CuBTC is to assign the FF associated with adsorbate−Cu interactions. We approached this task by performing extensive electronic structure calculations (specifically, dispersion corrected DFT calculations) of many configurations of molecules of interest in the fully periodic structure of the MOF and using the resulting data to fit a FF. By using the fully periodic structure of the MOF in our calculations, we avoid the possibility of cluster size effects, which may lead to unrealistic results. This approach has proven to be fruitful in a variety of recent studies of MOFs and zeolites.[48] Progress in this area has been reviewed recently.[37,49]

The force field development approach used here is similar to that of our previous work.[44] We first calculate the interaction energies for a few (<150) preferred adsorbate configurations using dispersion-corrected density functional theory (DFT). These interaction energies are fit to a classical potential form to obtain an initial FF. We use this FF in a grand canonical Monte Carlo (GCMC) simulation to generate isotherms and a larger set (300−600) of adsorbate configurations. DFT interaction energies are then obtained for the new configurations, and the FF parameters are recalculated using the full set of DFT data to yield the final, DFT-consistent version of the force field. Although we use a large number of DFT calculations to ensure that the entire configuration space is well represented by the FF, we later show that well-converged FF parameters can be obtained by using a much smaller subset of adsorbate configurations.

The initial crystal structure for CuBTC[39] was optimized at the DFT level using the dispersion-corrected PBE-D2[50,51] functional using the Vienna ab initio simulation package (VASP).[52,53] A plane wave cutoff of 700 eV was used to optimize the lattice constants, while the internal atomic positions are obtained at a lower 400 eV cutoff. The energy minimization is terminated when the individual atomic forces are less than 0.03 eV/Å. To reduce computational cost, the DFT calculations were performed at the Γ-point. The dicopper metal cluster in CuBTC is known to be antiferromagnetic,[54] and periodic calculations are initialized with the appropriate spin ordering. The PBE-D2-optimized lattice constants are in good agreement with experimental data (Table S1).

Our FF development approach is based on fitting the interaction energies obtained from periodic DFT calculations to a classical potential form. The interaction energy of the adsorbate molecule is defined as

$$E_{\text{interaction}} = E_{\text{MOF+ads}} - E_{\text{MOF}} - E_{\text{ads}} \quad (1)$$

where E_{MOF} and E_{ads} refer to the DFT energies of the empty CuBTC framework and the adsorbate molecule, respectively, while $E_{\text{MOF+ads}}$ is the DFT energy of the adsorbed hydrocarbon/MOF system. Because our FF is intended for use in GCMC calculations with a rigid MOF structure, adsorbate/MOF DFT energies were computed without any structural relaxation.

Our previous results for hydrocarbon adsorption in MIL-47(V) suggest that FFs derived from the VDW-DF2 functional of Langreth, Lundqvist, and co-workers[55] give better agreement with experimental isotherms than the PBE-D2[50,51] method. Similar DFT-based approaches have been used to model H_2, CO_2, and H_2O adsorption in the MOF-74 series.[18,35,56]

All GCMC simulations were performed with RASPA.[57,58] For adsorption simulations involving longer hydrocarbons, configurational-bias Monte Carlo (CBMC)[59] was employed. A 2 × 2 × 2 supercell of CuBTC was used and the pairwise interaction potentials were truncated at a spherical cutoff of 13.0 Å. Analytical tail corrections were included to model long-range dispersion interactions. CBMC calculations were equilibrated using at least 100000 cycles, and production runs of 400000 cycles were used for measuring adsorption properties.

3. RESULTS AND DISCUSSION

Ethane and Ethylene in CuBTC. We first discuss the application of our force field development methodology for modeling ethylene and ethane adsorption in CuBTC. Multiple configurations of an ethylene molecule were generated in CuBTC, as illustrated in Figure 1. To probe the interaction of the π-bond with the Cu OMS, ethylene was placed directly above the Cu atom such that (1) the center of the C═C double bond lies in the direction of the Cu−Cu vector (dotted green line), (2) the C═C double bond is perpendicular to the Cu−Cu vector, and (3) the plane of the ethylene molecule is normal to the Cu−Cu vector. The total DFT energy was calculated with 13 different distances between ethylene and the Cu atom. To better describe the interactions with the Cu OMS, 10 additional configurations are generated at each distance by randomly rotating the adsorbate about the Cu−Cu axis (θ, Figure 1). Ethane configurations were generated in a similar way. For generating the initial ethane configurations, an

DOI: 10.1021/acs.jpcc.6b07493
J. Phys. Chem. C 2016, 120, 23044−23054

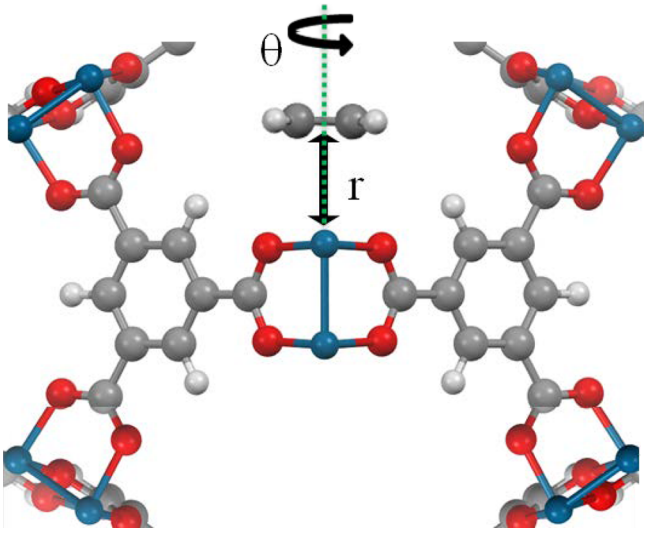

Figure 1. Orientations used for calculating the interaction energies of ethylene with the periodic CuBTC structure. The dotted green line represents the direction of the Cu−Cu vector. The color scheme used is C (gray), O (red), H (white), and Cu (blue).

additional random rotation about the C−C single bond is included to sample a wider configuration space arising due to the positions of the H atoms.

Figure 2 shows the minimum interaction energies among the configurations sampled at each distance for ethane and

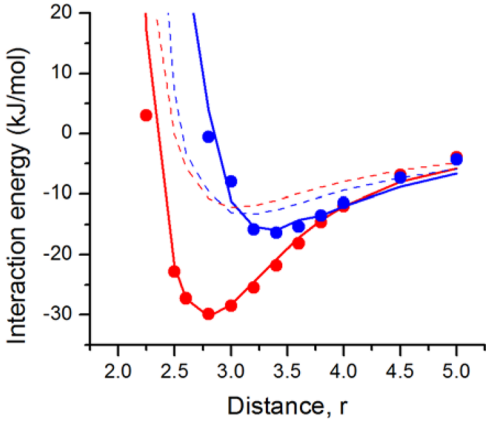

Figure 2. Interaction energies for initial configurations of ethane (blue) and ethylene (red) in CuBTC calculated using VDW-DF2 DFT (filled circles) and the fitted force field (solid lines). The dotted lines represent the contributions from the generic DREIDING FF for C, H, and O interactions.

ethylene. The most favorable configuration for ethylene is ∼2.8 Å from the Cu atom with an interaction energy of −29.9 kJ/mol. The ethane interactions are considerably weaker (−16.4 kJ/mol in the most favorable state) and are dominated by the dispersion interactions.[60]

The dotted curves in Figure 2 show the DREIDING/TraPPE FF contributions from interactions of the C, H, and O atoms with the adsorbates. It is clear that this generic FF gives a similar description of the non-Cu atoms for both adsorbates and that correctly describing the adsorbate interactions with Cu is crucial to describing these systems.

As discussed above, we assume that the DFT interaction energy can be decomposed into two parts

$$E_{\mathrm{DFT}} = E_{\mathrm{generic,non\text{-}Cu}} + E_{\mathrm{Cu\text{-}ads}} \tag{2}$$

where E_{DFT} is the total DFT interaction energy, $E_{\mathrm{generic,non\text{-}Cu}}$ is the contribution of the non-Cu atoms (H, C and O) calculated from DREIDING/TraPPE FF and $E_{\mathrm{Cu-ads}}$ is the interaction energy from the Cu OMS with the adsorbate. Using our DFT data and the generic FF contributions, we fitted $E_{\mathrm{Cu-ads}}$ to a pairwise Morse potential

$$U = D_0\left[\exp\left(\alpha\left(1-\frac{r}{\rho}\right)\right) - 2\exp\left(\frac{\alpha}{2}\left(1-\frac{r}{\rho}\right)\right)\right] \tag{3}$$

where D_0 is energy minimum, ρ is the distance corresponding to the energy minimum, and α indicates the curvature of the potential well. The least-squares fitted Morse parameters for ethane and ethylene are listed in Table S5. The solid curves in Figure 2 show the results of this FF, which we denote VDW-DF2 FF (iteration 1).

We examined the ability of this FF to predict adsorption in CuBTC by comparison with experimental data from Wang et al.[43] and Jorge et al.[12] at various temperatures. The experimental pore volume of the CuBTC sample used by Wang et al.[43] (0.658 cc/g) and Jorge et al.[12] (0.71 cc/g) is lower than the calculated pore volume for the ideal CuBTC material (0.84 cc/g) used in our GCMC simulations. To compare the GCMC isotherms with the experimental measurements, we scaled the experimental isotherms based on the ratio of the pore volumes of the ideal and the experimental crystal.[11,44]

Parts a and b of Figure 3 show the isotherms obtained when GCMC simulations are used with the VDW-DF2 (iteration 1) FF for ethane and ethylene, respectively. The GCMC predictions for ethane are in good agreement with the experimental isotherms at 295, 323, and 348 K, while a slight overestimation at 373 K is observed at higher pressures. Reasonable agreement with the scaled experimental data for ethylene is observed at lower partial pressures, and a slight overprediction is seen at the higher pressures. The deviation is more significant for the 295 K data of Wang et al.[38] In this case, the experimental data at 295 K approaches the 323 K isotherm at ∼88 kPa, suggesting incomplete equilibration at the lower temperature.[12]

We also computed isotherms using the generic DREIDING/TraPPE FF, including contributions from Cu atoms. The resulting isotherms are in moderately good agreement for ethane but severely underestimate ethylene adsorption (Figure S6). This supports previous observations that generic FFs cannot adequately describe adsorption of this kind in OMS MOFs.[15,40]

In addition, we performed an analogous set of calculations to Figures 1−3 using DFT data from the PBE-D2 functional (see Figures S2 and S3). Although the resulting ethane adsorption isotherms are in good agreement with the experimental data, ethylene adsorption is severely overestimated. This appears to be due to the overbinding of chemisorption energies by the PBE functional.[61] As the olefin isotherms are not correctly predicted using the PBE-D2 functional, we do not consider the PBE-D2 method in the remainder of this work.

Improved FFs for Ethane and Ethylene in CuBTC. The results above indicate that the VDW-DF2 (iteration 1) FF gives good agreement with the experimental ethane and ethylene isotherms. This FF, however, was obtained by only considering a limited set of favorable orientations of the adsorbate. For the

DOI: 10.1021/acs.jpcc.6b07493
J. Phys. Chem. C 2016, 120, 23044−23054

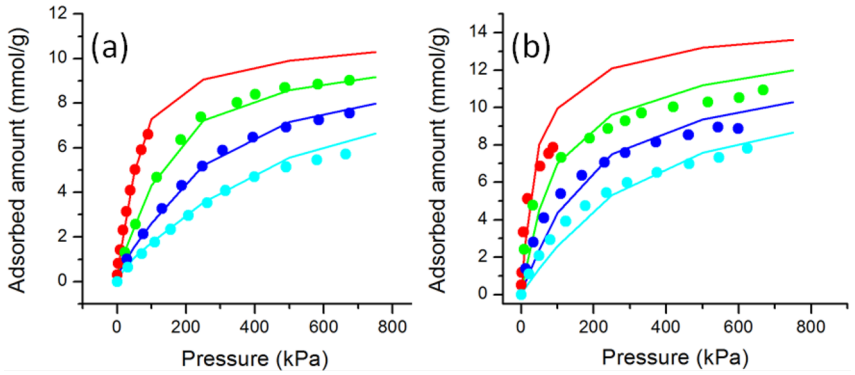

Figure 3. GCMC-predicted adsorption isotherms (solid curves) for (a) ethane and (b) ethylene in CuBTC using the VDW-DF2 (iteration 1) FF for the framework atoms and the TraPPE FF for the adsorbates at 295 K (red), 323 K (green), 348 K (blue), and 373 K (cyan). The scaled experimental adsorption isotherms from Wang et al.[43] at 295 K (red) and Jorge et al.[12] at 323 K (green), 348 K (blue), and 373 K(cyan) are shown by filled circles.

FF to be truly consistent with the underlying DFT calculations, we need to ensure that the DFT interaction energies for other configurations are also reproduced.[44]

Similar to our previous work,[44] we performed GCMC simulations (1 bar and 295 K) using the iteration 1 FF to generate a new set of configurations for ethane and ethylene. Periodic DFT calculations were performed to obtain the VDW-DF2 interaction energies for these new configurations. As the TraPPE hydrocarbon model only defines the CH3_sp3 and CH2_sp2 united atoms, it is necessary to add the appropriate hydrogen atoms prior to the DFT calculation. The constraints used for this purpose are summarized in Table S6.

Figure 4 compares the interaction energies for 300 configurations of ethane in CuBTC calculated using the

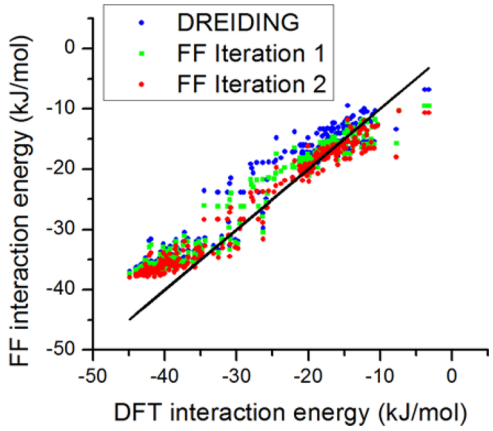

Figure 4. Comparison of the interaction energies calculated from VDW-DF2 DFT with the DREIDING FF (blue), VDW-DF2 (iteration 1) FF (green), and VDW-DF2 (iteration 2) FF (red) for 300 configurations of ethane in CuBTC.

VDW-DF2 method with the DREIDING FF and our DFT derived FFs. The mean absolute deviation (MAD) for the DREIDING FF (4.1 kJ/mol) is higher than the MAD for our iteration 1 FF (2.9 kJ/mol). Figure 4 also shows a systematic underestimation of ~10 kJ/mol for low energy configurations for ethane for both FFs. Note that for these configurations the adsorption energies (~−40 kJ/mol) are much lower than the most favorable values (~−15 kJ/mol) from Figure 2. This discrepancy is also seen for ethylene and will be discussed later.

Using the VDW-DF2 interaction energies for the new configurations, we refit the Morse potential parameters for ethane to obtain the second iteration of the VDW-DF2 FF. The fitted parameters for VDW-DF2 (iteration 2) FF are presented in Table S7. On using this FF, the MAD in Figure 4 decreases to ~2.4 kJ/mol, but the difference between the GCMC predicted isotherms with the two VDW-DF2 FFs is small (Figure S4). These results suggest that performing the second iteration did not significantly improve the capability of the FF to describe the DFT data for ethane. Nevertheless, this approach validates the reliability of the iteration 1 FF for predicting interaction energies of configurations that were not initially included above.

Similar calculations were performed for ethylene (Figure 5). The DREIDING FF fails at predicting the VDW-DF2 DFT

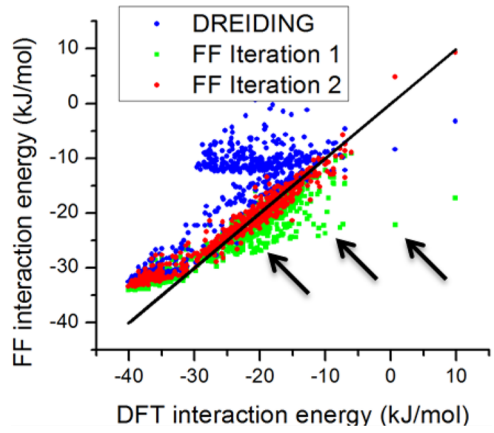

Figure 5. Comparison of the interaction energies calculated from the VDW-DF2 DFT method with the DREIDING FF (blue), VDW-DF2 (iteration 1) FF (green), and VDW-DF2 (iteration 2) FF (red) for 600 configurations of ethylene in CuBTC. The arrows indicate some of the configurations where the predicted energies from the iteration 1 FF are more negative than the VDW-DF2 predictions.

interaction energies (MAD = 7.9 kJ/mol). Compared to the DREIDING FF, a significantly improved prediction of DFT energies is observed for the iteration 1 FF (MAD = 3.2 kJ/mol). However, for a number of configurations (black arrows, Figure 5), the FF-predicted energies are much more negative than the VDW-DF2 curves in Figure 2.

DOI: 10.1021/acs.jpcc.6b07493
J. Phys. Chem. C 2016, 120, 23044−23054

Further analysis of the configurations highlighted in Figure 5 suggests that the deviation occurs due to pairwise potential used for interaction of the CH2_sp2 UA with the Cu OMS and the orientation of the ethylene molecule. Figure 6 shows two

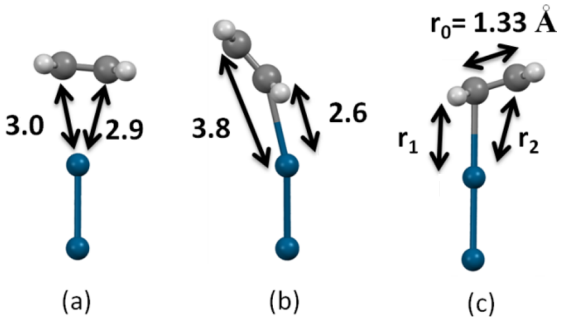

Figure 6. (a, b) Examples of ethylene configurations in CuBTC obtained from GCMC simulations at 295 K and 1 bar. (c) Notations used in eq 4. Only the Cu dimer closest to ethylene is shown for clarity. The color scheme is C (gray), O (red), H (white), and Cu (blue).

ethylene configurations obtained from GCMC simulations and their relative positions to the closest Cu OMS. The interaction energies calculated from VDW-DF2 and VDW-DF2 FF are shown in Table S8.

For the configuration shown in Figure 6a, the two C atoms of ethylene are essentially equidistant from the closest Cu atom. This orientation is similar to the initial configurations used in our initial DFT calculations for adsorbed ethylene. It is therefore not surprising that the interaction energy predicted from the VDW-DF2 FF is similar to the VDW-DF2 DFT value (−29.1 kJ/mol). Conversely, in Figure 6b, ethylene is tilted (r_1 = 2.6 Å and r_2 = 3.8 Å) and DFT predicts an unfavorable interaction (E_{DFT} = 9.8 kJ/mol) with the framework. Even though the average adsorbate−Cu distance is the same as in Figure 6a, a favorable π-bond/Cu OMS interaction is not possible in Figure 6b due to the orientation of the molecule. As the pairwise description of our FF only considers the individual distances of the C atoms with the Cu OMS (r_1 and r_2), the FF incorrectly predicts interaction energy of −17.0 kJ/mol.

Similar analysis of the individual r_1 and r_2 distances (see Figure 6c) and comparison of the interactions energies for 600 ethylene configurations suggest that an additional orientation-dependent term (denoted E_{orient}) is required to correctly account for this phenomenon. Since the orientation of the π-bond is most important for configurations close the Cu atom, the correction function should decay to small values far away from the Cu atom. Also, for ethylene orientations that are on top of the Cu atom (i.e., $r_1 - r_2 = 0$), the E_{orient} value must rapidly approach zero. From the surface plot presented in Figure S6, we determined that a nested exponential function

$$E_{orient} = 1 - \exp\left[A \exp(-Br_1)\left(\frac{r_1 - r_2}{r_0}\right)\right] \quad (4)$$

is suitable for describing the decaying nature of the required correction term. In eq 4, r_1 and r_2 are C−Cu distances, r_0 is the C−C bond length for ethylene (1.33 Å), and A and B are fitting parameters to be calculated. This orientation dependent energy is a three-body interaction that depends the positions of the two ethylene C atoms relative to the framework Cu atoms.

Using the difference in the interaction energies calculated from VDW-DF@ DFT and the VDW-DF2 (Iteration 1) FF, the parameters A and B were fitted (Table S9). The ethylene FF that includes the orientation-dependent energy term is denoted as the VDW-DF2 (iteration 2) FF. Table S8 shows that the interaction energies for the two configurations in Figure 6 calculated using the iteration 2 FF are in much better agreement with VDW-DF2 data. Figure 5 shows that the interaction energies calculated using the VDW-DF2 (iteration 2) FF (red circles) are in much better agreement with the VDW-DF2 DFT data. The overall MAD for iteration 2 FF (2.3 kJ/mol) is lower than the iteration 1 value (3.2 kJ/mol).

Figure S7 compares the MAD and mean deviation (MD) for the DREIDING, iteration 1, and iteration 2 ethylene FFs as a function of the distance from the Cu OMS. The DREIDING FF fails at predicting the interaction energies close to the Cu OMS (MAD = 12 kJ/mol). For distances shorter than 4.5 Å, the MAD for the iteration 2 FF is less than 2 kJ/mol, while the MD is close to zero. This is a significant improvement over the iteration 1 FF where MAD of ∼4 kJ/mol is seen for the same configurations. These results suggest that including the orientation dependent term considerably improved the quality of VDW-DF2 FF for the important configurations close to the Cu atom.

We now turn to addressing the systematic deviations previously observed in Figures 5 and 6 for ethane and ethylene adsorption in CuBTC for all the FFs we tested. This discrepancy is also seen in Figure S7 for larger ethylene−Cu distances (5−6 Å). For these cases, the ethylene molecule is present in the small octahedral pockets of CuBTC, resulting in interaction energies that are more negative than −30.0 kJ/mol (Figure S8). As the adsorbate/Cu distance is >5 Å, the interactions with the Cu atom are quite small and the generic DREIDING FF for C, H and O atoms dominates the total interaction energy. For these confined hydrocarbon configurations, the DREIDING FF underestimates the interaction energy by ∼5 kJ/mol relative to VDW-DF2 DFT, resulting in the deviations observed earlier. Despite these small deviations, good agreement with the experimental isotherms is observed as the octahedral cages are almost completely saturated under moderate pressures (see Figure S9 for discussion). However, we acknowledge that a more accurate description of this confined binding site will be essential when comparing low pressure data. One approach for resolving this discrepancy would be to reparametrize the DREIDING FF for these confined hydrocarbon configurations.[62] As the goal of this work is to parametrize the Cu−OMS interactions without altering the DREIDING FF, we do not explore this issue further.

To compute adsorption isotherms for ethylene using our iteration 2 FF, minor modifications to the RASPA simulation code[57,58] were required to incorporate the three-body nature of the E_{orient} calculation. Specifically, the MC scheme and the biasing factors were modified to incorporate E_{orient} while performing the translation, random translation, rotation, identity swap, and insertion/deletion moves. Comparing the isotherms computed with the iteration 1 and iteration 2 FFs shows that the ethylene adsorption isotherms from the two FFs are similar to each other (Figure S5). Analysis of the GCMC configurations, however, reveals important differences in the preferred adsorbate geometries of the two force fields. For both FFs, we used GCMC simulations at 295 K to obtain 5000 configurations of ethylene in CuBTC. The resulting distribution of angles, θ, formed between the C═C double bond and

DOI: 10.1021/acs.jpcc.6b07493
J. Phys. Chem. C 2016, 120, 23044−23054

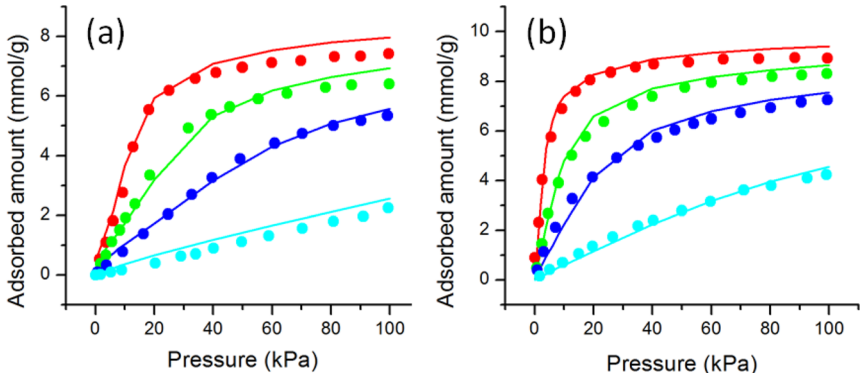

Figure 7. GCMC-predicted adsorption isotherms for (a) propane and (b) propylene in CuBTC using the VDW-DF2 (iteration 2) FF for the framework atoms and the TraPPE FF (solid lines) for the adsorbates at 323 K (red), 348 K (green), 373 K (blue), and 423 K (cyan). The scaled experimental adsorption isotherms from Fischer et al.[40] are shown by filled circles.

the vector connecting the Cu atom to the center of mass (COM) of ethylene is presented in Figure S10. Using this metric, we consider an adsorbate molecule with $\theta > 70°$ to be "flat" relative to the Cu atom and to have a favorable interaction of the π-bond with the Cu OMS. Our results show that at distances close to the Cu atom (<3 Å, black arrows in Figure S11) only ~50% of ethylene molecules are in the favorable "flat" orientation. However, when the orientation correction term is included (Figure S11b), close to 80% of the ethylene configurations are now "flat" relative to the Cu atom. For the configurations at longer distances from Cu, the influence of E_{orient} is not significant. Our results suggest that including the orientation term provides a more realistic olefin configuration close to the open metal sites and should be included in adsorption calculations. Further, on including E_{orient}, slight differences in ethane/ethylene selectivity are seen from binary GCMC calculations (Figure S12).

Force Fields for Propane and Propylene Adsorption in CuBTC. We extended the work above to develop similar FFs for propane and propylene adsorption in CuBTC. The ethane and ethylene results above define Morse FF parameters for CH2_sp2 UA (ethylene) and CH3_sp2 UA (ethane) interactions with the Cu OMS. To describe adsorption of propane and propylene, additional CH_sp2 (propylene) and CH2_sp2 (propane) interaction parameters are required. Methods similar to those described above were used to determine these parameters using VDW-DF2 energies from specific molecular configurations near Cu OMS and also configurations from GCMC simulations using an initial FF. It is encouraging to note that the our VDW-DF2 binding energies for propylene (−40 kJ/mol) are in better agreement with benchmark CCSD(T)/CBS predictions[60] (−41 kJ/mol) than the previously used PBE approach[12] (−33 kJ/mol). Further details are given in the Supporting Information.

Using the FF parameters in Table S10, we performed GCMC simulations for propane and propylene in CuBTC to generate adsorption isotherms at different temperatures. Parts a and b of Figure 7 compare the predicted propane and propylene isotherms with the experimental data of Fischer et al.[40] The experimental data was scaled to match the calculated pore volume of 0.85 cc/g. The predicted isotherms show excellent agreement with the experimental data for both propane and propylene.

Since we now have interaction parameters for CH3_sp3, CH2_sp3, CH2_sp2, and CH_sp2 with the Cu OMS, the DFT-derived VDW-DF2 FF can be used for modeling adsorption of higher olefins and paraffins.[44] As our FF is derived from VDW-DF2 calculations, we expect it to be transferable to other similar materials. We test this hypothesis in the next section.

Force Field Transferability to Other Cu Open Metal Site MOFs. Before using the FF developed above to computationally screen materials, it is necessary to examine the transferability of the FF parameters to other Cu OMS MOFs. In this section, we evaluate the transferability of our ethane and ethylene FF based on two independent metrics, namely (1) comparison of predicted and experimental isotherms and (2) comparison of the FF energies with DFT calculations for various MOFs.

Experimental data for olefin/paraffin adsorption in Cu OMS MOFs are limited, and reproducible isotherms from different groups are available only for CuBTC.[12,15,38] However, a previous study by He et al.[9] reported isotherms for a range of MOFs including MOF-505, PCN-16, UMCM-150, NOTT-101, NOTT-102, and USTA-20.[63−69] The experimental and calculated surface areas and pore volumes are summarized in Table S11. We compare the scaled experimental ethane and ethylene isotherms with the DREIDING and VDW-DF2 (iteration 2) FFs in Figure S15. The predicted isotherms using the VDW-DF2 FF tend to overpredict the adsorption isotherms. However, we note that the experimental measurements are limited to low temperatures and low pressures, and similar under-prediction is seen for CuBTC isotherms under such conditions (Figure 4). Surprisingly, comparable or higher ethane uptake is observed in many of the materials, suggesting that only a fraction of Cu sites are available for ethylene adsorption (see the discussion in Table S12). Although our FF gives results that are as consistent in these MOFs as in CuBTC, it is presumptuous to conclude that the FF is fully transferable at this stage. Instead, it would be useful to obtain additional experimental data to further examine these materials and FF predictions more thoroughly.

Noting the limited availability of reproducible experimental data for other MOFs, we explore an alternate approach to evaluate transferability by comparing the energetics predicted by our FF with periodic DFT calculations in related Cu−OMS MOFs. Because of the size of the unit cells of the materials listed above, periodic DFT calculations are feasible only for MOF-505 and PCN-16. In both these MOFs, the metal center consists of the dicopper cluster surrounded by octahedrally coordinated by eight oxygen atoms, similar to CuBTC. However, the linkers for MOF-505 (3,3′,5,5′-biphenyltetracar-

DOI: 10.1021/acs.jpcc.6b07493
J. Phys. Chem. C 2016, 120, 23044−23054

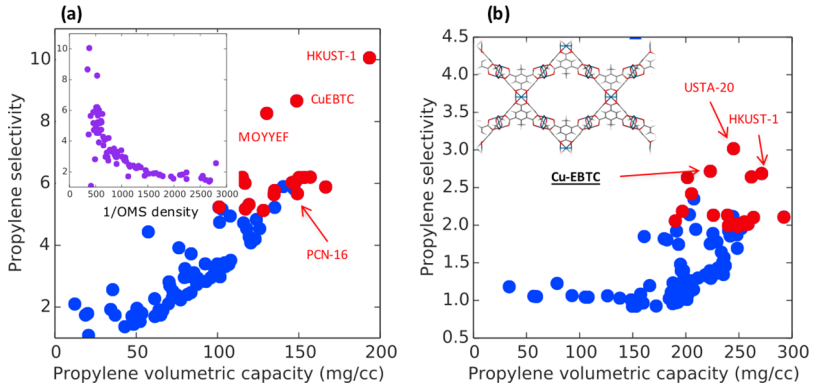

Figure 8. Propylene/propane selectivity and volumetric propylene capacity for (a) 10/90 and (b) 50/50 bulk mixtures for 94 dicopper OMS containing MOFs (blue circles). The red circles represent the 18 MOFs that have the highest selectivities (top 25) for both mixtures. The inset in (a) indicates the correlation of propylene/propane selectivity with the density of OMS. The inset in (b) shows one channel of Cu-EBTC lined with Cu OMS.

boxyl)[64] and PCN-16 (5,5′-ethyne-1,2-diyldiisophthalato)[63] differ from the CuBTC linker (1,3,5-benzenetricarboxylate).[39] Similar to our calculations in section 2, initial favorable configurations for ethane and ethylene were generated in MOF-505 and PCN-16. The DFT interaction energies calculated with the VDW-DF2 functional are compared to VDW-DF2 FF predictions in Figure S16. The FF derived from CuBTC gives excellent predictions for the energies of both molecules in MOF-505 and PCN-16.

We also evaluated the transferability of the orientation-dependent term fitted to CuBTC for MOF-505 and PCN-16. A set of ethylene configurations were obtained from GCMC snapshots and were used for periodic DFT calculations using VDW-DF2. The DFT interaction energies for 400 GCMC-generated configurations are compared with the DREIDING and VDW-DF2 FF predictions in Figure S17 for MOF-505 and PCN-16. As the interactions of the Cu OMS are not represented correctly, the DREIDING FF fails at predicting the VDW-DF2 interaction energies. The VDW-DF2 (iteration 1) FF gives reasonable agreement with the DFT energies but substantially overpredicts the interaction energies for some of the configurations due to the unfavorable orientations of ethylene close to the Cu OMS. Not surprisingly, the best performance is seen for the Iteration 2 VDW-DF2 FF that includes the orientation correction. The MAD for the interaction energies obtained from Iteration 2 FF for MOF-505 (2.1 kJ/mol) and PCN-16 (1.7 kJ/mol) are actually lower than the CuBTC results (2.3 kJ/mol). We attribute this observation to the absence of the confinement effect previously discussed for octahedral side-pockets in CuBTC.

Throughout the calculations described in this section the parameters used for the VDW-DF2 FF were obtained from CuBTC results in section 2 and were not reparameterized for the new systems. Our results thus provide strong evidence that our VDW-DF2 FF is transferable to MOFs with Cu OMS.

Screening of MOFs with Open Cu Sites for Propane/Propylene Separations. Having shown that our DFT-derived FF is transferable among MOFs with Cu OMS, we now turn to using this FF to screen materials for separations of practical interest. Although MOFs with other coordinatively unsaturated metals have been shown to be useful for olefin/paraffin separations,[9,70,71] FF development for other metal centers is beyond the scope of this work. We used the algorithm described in Table S13 to automatically detect MOFs with open Cu sites from the materials listed in the CoRE MOF database of Chung et al.[72] We have previously used a similar approach to screen Cu−MOFs for desirable electrical properties.[73] Since the FF has been developed for metal centers that consist of Cu dimers surrounded by eight neighboring atoms, we restrict our search to finding MOFs with similar Cu connectivities. The set of 94 MOF structures identified by this analysis are summarized in Table S14. This list includes the MOFs previously studied experimentally by He et al.[9]

To examine the viability of these materials for equilibrium propane/propylene separations, we chose volumetric propylene capacity (mg/cm^3-adsorbate) and propylene/propane selectivity as metrics for determining separation performance.[29] Specifically, for each MOF we performed a binary GCMC simulation using 50/50 and 10/90 bulk propylene/propane mixtures (303 K, total pressure 2.5 bar). Figure 8 shows the results for the two mixtures. For the 10/90 mixture, there is a favorable correlation between the selectivity and the propylene volumetric capacity due to the preferential adsorption of propylene at the Cu sites. For the equimolar mixtures, the OMS are saturated by propylene (Figure 8b), and physisorption of both components reduces the overall selectivity. A strong correlation between selectivity and volumetric density of Cu OMS (Figure 8a, inset) suggests that MOFs having small fractions of nonselective volumes are desirable. In contrast to gas storage applications where large internal pore volumes are desirable,[16,74] relatively low pore volume materials with a high density of Cu sites are necessary for improved olefin/paraffin selectivity.

Using the data in Figure 8, we found the 25 MOFs with the highest selectivity for each gas-phase mixture. Among these materials, 18 MOFs are in the top performing for both mixtures and are summarized in Table 1 and Table S15. It is encouraging that this includes some well-studied MOFs such as CuBTC (refcode FIQCEN), Cu-EBTC[75] (refcode LAZXOB), and PCN-16 (refcode NUTQEZ). The correlation of selectivity with open metal site density is especially interesting and provides a simple metric for identifying other MOFs suitable for this separation that may not been included here.

The results above are based on GCMC simulations of adsorbed mixtures at only two specific conditions. To further analyze materials of interest, it is useful to characterize their binary adsorption isotherms more completely. As the systematic experimental measurement of binary isotherms for different

DOI: 10.1021/acs.jpcc.6b07493
J. Phys. Chem. C 2016, 120, 23044−23054

Table 1. Volumetric Capacity and Propylene Selectivity of Top-Performing Dicopper OMS-Containing MOFs Identified from the Screening Analysis for 10/90 Propylene Mixtures

REFCODE	volumetric capacity (mg/cm^3)	propylene selectivity
FIQCEN (HKUST-1)	193.5	10.1
LAZXOB (Cu-EBTC)	148.7	8.7
MOYYEF	130.3	8.3
NUTQEZ (PCN-16)	157.0	6.2
XOPLOE	115.2	6.2
MOCKAR	153.3	6.2
BEXVEH	150.1	6.2
NUTQAV (PCN-16′)	148.0	6.1
MAFJIO	145.8	6.0
PARNON	116.9	6.0
HOGLEV	166.5	5.9
XITYOP	135.1	5.8
LASDEQ	149.1	5.7
LASYOU (MOF-505)	134.7	5.6
HANWAW	119.3	5.3
YEKXOD	101.0	5.2
ONIXOZ (USTA-20)	117.2	5.2
FECXES	128.2	5.1

[a]Further details are presented in Table S15.

gas compositions is challenging, the ideal adsorbed solution theory (IAST) is frequently used as an approximation.[76,77] Using only the pure component adsorption isotherms (experimental or predicted), IAST predicts the binary isotherms that can be used, for example, in a process model. This approach has been used, for example, by He et al. to evaluate MOFs for various hydrocarbon separations.[9] However, IAST may not be accurate for systems with inhomogeneous adsorption sites, strong interactions with some adsorbates, or other nonidealities. As the interaction of propylene with Cu OMS is specific in nature, we examined the applicability of IAST for the Cu OMS MOFs using CuBTC as an example.

We used binary GCMC simulations with our VDW-DF2 FF to predict the mixture adsorption of propylene and propane in CuBTC at a wide range of bulk pressures and compositions at 303 K (Figure S18). A single site Toth model was fit to the single component isotherms (Figure S19), and IAST was then used to predict the binary adsorption of propane and propylene. As shown in Figure S20, the IAST predictions are in reasonable agreement with the GCMC data for propylene, but IAST underpredicts propane adsorption. As a result, IAST systematically overpredicts the propylene/propane selectivity in CuBTC. This systematic shortcoming of IAST is not unique to CuBTC. We performed similar calculations for each of the other 17 MOFs listed in Table 1. These calculations show that IAST does not give accurate predictions for these OMS MOFs.

The inaccuracy of IAST for these materials creates a challenge for constructing realistic process models for these materials. To aid future work on this topic, we systematically generated binary adsorption data using GCMC for propane/propylene mixtures for the 18 top-performing MOFs identified above. Specifically, for each MOF, binary GCMC simulations were performed at two temperatures (303 and 373 K), five gas phase compositions (0.0, 0.2, 0.5, 0.8, 1.0), and pressures ranging from 0.1 to 5 bar. This data set of equilibrium binary adsorption data for 6000 state-points is available in the Supporting Information.

4. CONCLUSIONS

We have introduced a force field for modeling adsorption of olefins and paraffins in MOFs containing open Cu sites. By performing numerous single-point energy calculations using periodic DFT with the VDW-DF2 functional, we developed a transferable force field that successfully predicts adsorption of ethane and ethene in CuBTC. Similar to our previous work with alkane adsorption in the MIL series,[44] we extended this force field to describe propane and propylene adsorption. As the interaction of the olefins with the open metal sites has a preferred geometry, we introduced a 3-body orientation dependent term that accounts for this behavior. This force field, denoted VDW-DF2 FF, shows excellent prediction of the experimental adsorption data for ethane, propane, ethylene and propylene adsorption over a wide range of temperatures. Although the FF was developed using data from a single MOF (CuBTC), we demonstrated that it is transferable to other MOFs containing open Cu sites.

Using an algorithm to efficiently identify OMS MOFs, we have used our FF to examine a collection of 94 Cu OMS MOFs for selective adsorption of propylene/propane mixtures. These calculations greatly extend the number of materials for which accurate data for adsorption of this mixture is available. This work identified a number of materials that appear to have good properties for this industrially interesting separation. The approach we have used is well suited to be applied to related olefin/paraffin separations in Cu OMS MOFs and to MOFs with other under-coordinated metal sites.

A key factor in the selective adsorption of propylene over propane in Cu OMS MOFs is the specific interactions that occur between propylene and the open Cu sites. While this interaction makes the materials selective, it also means that theories of mixture adsorption based on assumptions of ideal mixing such as IAST do not give accurate predictions for these materials. In this case, material screening and process modeling studies based on single component adsorption isotherms and IAST approximation for mixtures may no longer be suitable, and more complex analysis may be necessary. We have reported a large collection of mixture isotherm data for propane/propylene mixtures for the high-performing materials identified in our screening calculations. This data will be useful in future efforts to construct realistic process models of cyclic adsorption processes using these materials and, more generally, in the development of adsorption mixing theories suitable for adsorbents where specific interactions are central to a material's separation performance.

■ ASSOCIATED CONTENT

Supporting Information

The Supporting Information is available free of charge on the ACS Publications website at DOI: 10.1021/acs.jpcc.6b07493.

Binary isotherms from GCMC simulations (ZIP)

Details of the force field development methodology (PDF)

■ AUTHOR INFORMATION

Corresponding Author

*E-mail: david.sholl@chbe.gatech.edu. Tel: 404-894-2822.

DOI: 10.1021/acs.jpcc.6b07493
J. Phys. Chem. C 2016, 120, 23044−23054

Notes

The authors declare no competing financial interest.

■ ACKNOWLEDGMENTS

We thank the ExxonMobil Chemical Co. for financially supporting this research. Useful discussions with Dr. Hanjun Fang, Dr. Jason Gee, and Dr. Rohan Awati are gratefully acknowledged.

■ REFERENCES

(1) Hydrocarbon Gas Liquids (Hgl): Recent Market Trends and Issues. http://www.eia.gov/analysis/hgl/pdf/hgl.pdf (accessed Sep 16, 2016).
(2) Growing U.S. Hgl Production Spurs Petrochemical Industry Investment. http://www.eia.gov/todayinenergy/detail.cfm?id=19771 (accessed Sep 16, 2016).
(3) Bloch, E. D.; Queen, W. L.; Krishna, R.; Zadrozny, J. M.; Brown, C. M.; Long, J. R. Hydrocarbon Separations in a Metal-Organic Framework with Open Iron(II) Coordination Sites. *Science* **2012**, *335*, 1606−1610.
(4) Herm, Z. R.; Bloch, E. D.; Long, J. R. Hydrocarbon Separations in Metal−Organic Frameworks. *Chem. Mater.* **2014**, *26*, 323−338.
(5) Eldridge, R. B. Olefin/Paraffin Separation Technology: A Review. *Ind. Eng. Chem. Res.* **1993**, *32*, 2208−2212.
(6) Sholl, D. S.; Lively, R. P. Seven Chemical Separations to Change the World. *Nature* **2016**, *532*, 435−437.
(7) Yaghi, O. M.; O'Keeffe, M.; Ockwig, N. W.; Chae, H. K.; Eddaoudi, M.; Kim, J. Reticular Synthesis and the Design of New Materials. *Nature* **2003**, *423*, 705−714.
(8) Krishna, R.; van Baten, J. M. In Silico Screening of Metal-Organic Frameworks in Separation Applications. *Phys. Chem. Chem. Phys.* **2011**, *13*, 10593−10616.
(9) He, Y.; Krishna, R.; Chen, B. Metal-Organic Frameworks with Potential for Energy-Efficient Adsorptive Separation of Light Hydrocarbons. *Energy Environ. Sci.* **2012**, *5*, 9107−9120.
(10) He, Y.; Zhou, W.; Krishna, R.; Chen, B. Microporous Metal-Organic Frameworks for Storage and Separation of Small Hydrocarbons. *Chem. Commun.* **2012**, *48*, 11813−11831.
(11) Fischer, M.; Gomes, J. R. B.; Jorge, M. Computational Approaches to Study Adsorption in MOFs with Unsaturated Metal Sites. *Mol. Simul.* **2014**, *40*, 537−556.
(12) Jorge, M.; Fischer, M.; Gomes, J. R. B.; Siquet, C.; Santos, J. C.; Rodrigues, A. E. Accurate Model for Predicting Adsorption of Olefins and Paraffins on Mofs with Open Metal Sites. *Ind. Eng. Chem. Res.* **2014**, *53*, 15475−15478.
(13) Furukawa, H.; Cordova, K. E.; O'Keeffe, M.; Yaghi, O. M. The Chemistry and Applications of Metal-Organic Frameworks. *Science* **2013**, *341*, 1230444.
(14) Li, J.-R.; Kuppler, R. J.; Zhou, H.-C. Selective Gas Adsorption and Separation in Metal-Organic Frameworks. *Chem. Soc. Rev.* **2009**, *38*, 1477−1504.
(15) Fischer, M.; Kuchta, B.; Firlej, L.; Hoffmann, F.; Fröba, M. Accurate Prediction of Hydrogen Adsorption in Metal−Organic Frameworks with Unsaturated Metal Sites Via a Combined Density-Functional Theory and Molecular Mechanics Approach. *J. Phys. Chem. C* **2010**, *114*, 19116−19126.
(16) Han, S. S.; Goddard, W. A. High H2 Storage of Hexagonal Metal−Organic Frameworks from First-Principles-Based Grand Canonical Monte Carlo Simulations. *J. Phys. Chem. C* **2008**, *112*, 13431−13436.
(17) Dzubak, A. L.; Lin, L. C.; Kim, J.; Swisher, J. A.; Poloni, R.; Maximoff, S. N.; Smit, B.; Gagliardi, L. Ab Initio Carbon Capture in Open-Site Metal-Organic Frameworks. *Nat. Chem.* **2012**, *4*, 810−816.
(18) Lin, L.-C.; Lee, K.; Gagliardi, L.; Neaton, J. B.; Smit, B. Force-Field Development from Electronic Structure Calculations with Periodic Boundary Conditions: Applications to Gaseous Adsorption and Transport in Metal−Organic Frameworks. *J. Chem. Theory Comput.* **2014**, *10*, 1477−1488.
(19) Han, S. S.; Kim, D.; Jung, D. H.; Cho, S.; Choi, S.-H.; Jung, Y. Accurate Ab Initio-Based Force Field for Predictive Co2 Uptake Simulations in MOFs and ZIFs: Development and Applications for MTV-MOFs. *J. Phys. Chem. C* **2012**, *116*, 20254−20261.
(20) Li, W.; Grimme, S.; Krieg, H.; Möllmann, J.; Zhang, J. Accurate Computation of Gas Uptake in Microporous Organic Molecular Crystals. *J. Phys. Chem. C* **2012**, *116*, 8865−8871.
(21) Chen, L.; Morrison, C. A.; Düren, T. Improving Predictions of Gas Adsorption in Metal−Organic Frameworks with Coordinatively Unsaturated Metal Sites: Model Potentials, Ab Initio Parameterization, and GCMC Simulations. *J. Phys. Chem. C* **2012**, *116*, 18899−18909.
(22) Chen, L.; Grajciar, L.; Nachtigall, P.; Düren, T. Accurate Prediction of Methane Adsorption in a Metal−Organic Framework with Unsaturated Metal Sites by Direct Implementation of an Ab Initio Derived Potential Energy Surface in GCMC Simulation. *J. Phys. Chem. C* **2011**, *115*, 23074−23080.
(23) Zang, J.; Nair, S.; Sholl, D. S. Prediction of Water Adsorption in Copper-Based Metal−Organic Frameworks Using Force Fields Derived from Dispersion-Corrected DFT Calculations. *J. Phys. Chem. C* **2013**, *117*, 7519−7525.
(24) Colon, Y. J.; Snurr, R. Q. High-Throughput Computational Screening of Metal-Organic Frameworks. *Chem. Soc. Rev.* **2014**, *43*, 5735−5749.
(25) Bae, Y.-S.; Snurr, R. Q. Optimal Isosteric Heat of Adsorption for Hydrogen Storage and Delivery Using Metal−Organic Frameworks. *Microporous Mesoporous Mater.* **2010**, *132*, 300−303.
(26) Fischer, M.; Hoffmann, F.; Fröba, M. Preferred Hydrogen Adsorption Sites in Various MOFs—a Comparative Computational Study. *ChemPhysChem* **2009**, *10*, 2647−2657.
(27) Mu, W.; Liu, D.; Yang, Q.; Zhong, C. Computational Study of the Effect of Organic Linkers on Natural Gas Upgrading in Metal−Organic Frameworks. *Microporous Mesoporous Mater.* **2010**, *130*, 76−82.
(28) Babarao, R.; Jiang, J.; Sandler, S. I. Molecular Simulations for Adsorptive Separation of Co2/Ch4Mixture in Metal-Exposed, Catenated, and Charged Metal−Organic Frameworks. *Langmuir* **2009**, *25*, 5239−5247.
(29) Haldoupis, E.; Nair, S.; Sholl, D. S. Finding Mofs for Highly Selective Co2/N2 Adsorption Using Materials Screening Based on Efficient Assignment of Atomic Point Charges. *J. Am. Chem. Soc.* **2012**, *134*, 4313−4323.
(30) Wilmer, C. E.; Leaf, M.; Lee, C. Y.; Farha, O. K.; Hauser, B. G.; Hupp, J. T.; Snurr, R. Q. Large-Scale Screening of Hypothetical Metal−Organic Frameworks. *Nat. Chem.* **2011**, *4*, 83−89.
(31) Yazaydın, A. Ö.; Snurr, R. Q.; Park, T.-H.; Koh, K.; Liu, J.; LeVan, M. D.; Benin, A. I.; Jakubczak, P.; Lanuza, M.; Galloway, D. B.; et al. Screening of Metal−Organic Frameworks for Carbon Dioxide Capture from Flue Gas Using a Combined Experimental and Modeling Approach. *J. Am. Chem. Soc.* **2009**, *131*, 18198−18199.
(32) Dzubak, A. L.; Lin, L.-C.; Kim, J.; Swisher, J. A.; Poloni, R.; Maximoff, S. N.; Smit, B.; Gagliardi, L. Ab Initio Carbon Capture in Open-Site Metal−Organic Frameworks. *Nat. Chem.* **2012**, *4*, 810−816.
(33) Ozturk, T. N.; Keskin, S. Computational Screening of Porous Coordination Networks for Adsorption and Membrane-Based Gas Separations. *J. Phys. Chem. C* **2014**, *118*, 13988−13997.
(34) Grajciar, L.; Bludsky, O.; Nachtigall, P. Water Adsorption on Coordinatively Unsaturated Sites in CuBTC MOF. *J. Phys. Chem. Lett.* **2010**, *1*, 3354−3359.
(35) Rudenko, A. N.; Bendt, S.; Keil, F. J. Multiscale Modeling of Water in Mg-MOF-74: From Electronic Structure Calculations to Adsorption Isotherms. *J. Phys. Chem. C* **2014**, *118*, 16218−16227.
(36) Haldoupis, E.; Borycz, J.; Shi, H.; Vogiatzis, K. D.; Bai, P.; Queen, W. L.; Gagliardi, L.; Siepmann, J. I. Ab Initio Derived Force Fields for Predicting Co2 Adsorption and Accessibility of Metal Sites in the Metal−Organic Frameworks M-MOF-74 (M = Mn, Co, Ni, Cu). *J. Phys. Chem. C* **2015**, *119*, 16058−16071.
(37) Fang, H.; Demir, H.; Kamakoti, P.; Sholl, D. S. Recent Developments in First-Principles Force Fields for Molecules in Nanoporous Materials. *J. Mater. Chem. A* **2014**, *2*, 274−291.

DOI: 10.1021/acs.jpcc.6b07493
J. Phys. Chem. C 2016, 120, 23044−23054

(38) Min Wang, Q.; Shen, D. M.; Bulow, M.; Ling Lau, M.; Deng, S. G.; Fitch, F. R.; Lemcoff, N. O.; Semanscin, J. Metallo-Organic Molecular Sieve for Gas Separation and Purification. *Microporous Mesoporous Mater.* **2002**, *55*, 217−230.
(39) Chui, S. S.-Y.; Lo, S. M.-F.; Charmant, J. P. H.; Orpen, A. G.; Williams, I. D. A Chemically Functionalizable Nanoporous Material [Cu3(TMA)2(H2O)3]N. *Science* **1999**, *283*, 1148−1150.
(40) Fischer, M.; Gomes, J. R. B.; Froeba, M.; Jorge, M. Modeling Adsorption in Metal-Organic Frameworks with Open Metal Sites: Propane/Propylene Separations. *Langmuir* **2012**, *28*, 8537−8549.
(41) Lamia, N.; Jorge, M.; Granato, M. A.; Almeida Paz, F. A.; Chevreau, H.; Rodrigues, A. E. Adsorption of Propane, Propylene and Isobutane on a Metal−Organic Framework: Molecular Simulation and Experiment. *Chem. Eng. Sci.* **2009**, *64*, 3246−3259.
(42) Nicholson, T.; Bhatia, S. Role of Electrostatic Effects in the Pure Component and Binary Adsorption of Ethylene and Ethane in Cu−Tricarboxylate Metal-Organic Frameworks. *Adsorpt. Sci. Technol.* **2007**, *25*, 607−619.
(43) Wang, S.; Yang, Q.; Zhong, C. Adsorption and Separation of Binary Mixtures in a Metal-Organic Framework Cu-BTC: A Computational Study. *Sep. Purif. Technol.* **2008**, *60*, 30−35.
(44) Kulkarni, A. R.; Sholl, D. S. DFT-Derived Force Fields for Modeling Hydrocarbon Adsorption in MIL-47(V). *Langmuir* **2015**, *31*, 8453−8468.
(45) Jorge, M.; Lamia, N.; Rodrigues, A. E. Molecular Simulation of Propane/Propylene Separation on the Metal−Organic Framework Cubtc. *Colloids Surf., A* **2010**, *357*, 27−34.
(46) Mayo, S. L.; Olafson, B. D.; Goddard, W. A. Dreiding - a Generic Force-Field for Molecular Simulations. *J. Phys. Chem.* **1990**, *94*, 8897−8909.
(47) Martin, M. G.; Siepmann, J. I. Transferable Potentials for Phase Equilibria. 1. United-Atom Description of n-Alkanes. *J. Phys. Chem. B* **1998**, *102*, 2569−2577.
(48) Fang, H.; Kulkarni, A.; Kamakoti, P.; Awati, R.; Ravikovitch, P. I.; Sholl, D. S. Identification of High CO2 Capacity Cationic Zeolites by Accurate Computational Screening. *Chem. Mater.* **2016**, *28*, 3887−3896.
(49) Odoh, S. O.; Cramer, C. J.; Truhlar, D. G.; Gagliardi, L. Quantum-Chemical Characterization of the Properties and Reactivities of Metal−Organic Frameworks. *Chem. Rev.* **2015**, *115*, 6051−6111.
(50) Perdew, J. P.; Burke, K.; Ernzerhof, M. Generalized Gradient Approximation Made Simple. *Phys. Rev. Lett.* **1996**, *77*, 3865−3868.
(51) Grimme, S. Semiempirical Gga-Type Density Functional Constructed with a Long-Range Dispersion Correction. *J. Comput. Chem.* **2006**, *27*, 1787−1799.
(52) Kresse, G.; Furthmüller, J. Efficient Iterative Schemes for Ab Initio Total-Energy Calculations Using a Plane-Wave Basis Set. *Phys. Rev. B: Condens. Matter Mater. Phys.* **1996**, *54*, 11169−11186.
(53) Kresse, G.; Joubert, D. From Ultrasoft Pseudopotentials to the Projector Augmented-Wave Method. *Phys. Rev. B: Condens. Matter Mater. Phys.* **1999**, *59*, 1758−1775.
(54) Watanabe, T.; Sholl, D. S. Molecular Chemisorption on Open Metal Sites in Cu3(Benzenetricarboxylate)2: A Spatially Periodic Density Functional Theory Study. *J. Chem. Phys.* **2010**, *133*, 094509.
(55) Lee, K.; Murray, É. D.; Kong, L.; Lundqvist, B. I.; Langreth, D. C. Higher-Accuracy van der Waals Density Functional. *Phys. Rev. B: Condens. Matter Mater. Phys.* **2010**, *82*, 081101.
(56) Borycz, J.; Lin, L.-C.; Bloch, E. D.; Kim, J.; Dzubak, A. L.; Maurice, R.; Semrouni, D.; Lee, K.; Smit, B.; Gagliardi, L. CO2 Adsorption in Fe2(DOBDC): A Classical Force Field Parameterized from Quantum Mechanical Calculations. *J. Phys. Chem. C* **2014**, *118*, 12230−12240.
(57) Dubbeldam, D.; Torres-Knoop, A.; Walton, K. S. On the Inner Workings of Monte Carlo Codes. *Mol. Simul.* **2013**, *39*, 1253−1292.
(58) Dubbeldam, D.; Calero, S.; Ellis, D. E.; Snurr, R. Q. RASPA: Molecular Simulation Software for Adsorption and Diffusion in Flexible Nanoporous Materials. *Mol. Simul.* **2016**, *42*, 81−101.
(59) Siepmann, J. I.; Frenkel, D. Configurational Bias Monte-Carlo - a New Sampling Scheme for Flexible Chains. *Mol. Phys.* **1992**, *75*, 59−70.
(60) Rubes, M.; Wiersum, A. D.; Llewellyn, P. L.; Grajciar, L.; Bludsky, O.; Nachtigall, P. Adsorption of Propane and Propylene on CuBTC Metal-Organic Framework: Combined Theoretical and Experimental Investigation. *J. Phys. Chem. C* **2013**, *117*, 11159−11167.
(61) Hammer, B.; Hansen, L. B.; Nørskov, J. K. Improved Adsorption Energetics within Density-Functional Theory Using Revised Perdew-Burke-Ernzerhof Functionals. *Phys. Rev. B: Condens. Matter Mater. Phys.* **1999**, *59*, 7413−7421.
(62) Hulvey, Z.; Vlaisavljevich, B.; Mason, J. A.; Tsivion, E.; Dougherty, T. P.; Bloch, E. D.; Head-Gordon, M.; Smit, B.; Long, J. R.; Brown, C. M. Critical Factors Driving the High Volumetric Uptake of Methane in Cu3(BTC)2. *J. Am. Chem. Soc.* **2015**, *137*, 10816−10825.
(63) Sun, D.; Ma, S.; Simmons, J. M.; Li, J.-R.; Yuan, D.; Zhou, H.-C. An Unusual Case of Symmetry-Preserving Isomerism. *Chem. Commun.* **2010**, *46*, 1329−1331.
(64) Hu, Y.; Xiang, S.; Zhang, W.; Zhang, Z.; Wang, L.; Bai, J.; Chen, B. A New MOF-505 Analog Exhibiting High Acetylene Storage. *Chem. Commun.* **2009**, 7551−7553.
(65) Lin, X.; Jia, J.; Zhao, X.; Thomas, K. M.; Blake, A. J.; Walker, G. S.; Champness, N. R.; Hubberstey, P.; Schröder, M. High H2 Adsorption by Coordination-Framework Materials. *Angew. Chem., Int. Ed.* **2006**, *45*, 7358−7364.
(66) Lin, X.; Telepeni, I.; Blake, A. J.; Dailly, A.; Brown, C. M.; Simmons, J. M.; Zoppi, M.; Walker, G. S.; Thomas, K. M.; Mays, T. J.; et al. High Capacity Hydrogen Adsorption in Cu(II) Tetracarboxylate Framework Materials: The Role of Pore Size, Ligand Functionalization, and Exposed Metal Sites. *J. Am. Chem. Soc.* **2009**, *131*, 2159−2171.
(67) Guo, Z.; Wu, H.; Srinivas, G.; Zhou, Y.; Xiang, S.; Chen, Z.; Yang, Y.; Zhou, W.; O'Keeffe, M.; Chen, B. A Metal−Organic Framework with Optimized Open Metal Sites and Pore Spaces for High Methane Storage at Room Temperature. *Angew. Chem., Int. Ed.* **2011**, *50*, 3178−3181.
(68) Chen, B.; Ockwig, N. W.; Millward, A. R.; Contreras, D. S.; Yaghi, O. M. High H2 Adsorption in a Microporous Metal−Organic Framework with Open Metal Sites. *Angew. Chem., Int. Ed.* **2005**, *44*, 4745−4749.
(69) Wong-Foy, A. G.; Lebel, O.; Matzger, A. J. Porous Crystal Derived from a Tricarboxylate Linker with Two Distinct Binding Motifs. *J. Am. Chem. Soc.* **2007**, *129*, 15740−15741.
(70) Bae, Y.-S.; Lee, C. Y.; Kim, K. C.; Farha, O. K.; Nickias, P.; Hupp, J. T.; Nguyen, S. T.; Snurr, R. Q. High Propene/Propane Selectivity in Isostructural Metal−Organic Frameworks with High Densities of Open Metal Sites. *Angew. Chem., Int. Ed.* **2012**, *51*, 1857−1860.
(71) Geier, S. J.; Mason, J. A.; Bloch, E. D.; Queen, W. L.; Hudson, M. R.; Brown, C. M.; Long, J. R. Selective Adsorption of Ethylene over Ethane and Propylene over Propane in the Metal-Organic Frameworks M2(DOBDC) (M = Mg, Mn, Fe, Co, Ni, Zn). *Chem. Sci.* **2013**, *4*, 2054−2061.
(72) Chung, Y. G.; Camp, J.; Haranczyk, M.; Sikora, B. J.; Bury, W.; Krungleviciute, V.; Yildirim, T.; Farha, O. K.; Sholl, D. S.; Snurr, R. Q. Computation-Ready, Experimental Metal−Organic Frameworks: A Tool to Enable High-Throughput Screening of Nanoporous Crystals. *Chem. Mater.* **2014**, *26*, 6185−6192.
(73) Nie, X.; Kulkarni, A.; Sholl, D. S. Computational Prediction of Metal Organic Frameworks Suitable for Molecular Infiltration as a Route to Development of Conductive Materials. *J. Phys. Chem. Lett.* **2015**, *6*, 1586−1591.
(74) Simon, C. M.; Kim, J.; Gomez-Gualdron, D. A.; Camp, J. S.; Chung, Y. G.; Martin, R. L.; Mercado, R.; Deem, M. W.; Gunter, D.; Haranczyk, M.; et al. The Materials Genome in Action: Identifying the Performance Limits for Methane Storage. *Energy Environ. Sci.* **2015**, *8*, 1190−1199.

DOI: 10.1021/acs.jpcc.6b07493
J. Phys. Chem. C 2016, 120, 23044−23054

(75) Cai, Y.; Kulkarni, A. R.; Huang, Y.-G.; Sholl, D. S.; Walton, K. S. Control of Metal−Organic Framework Crystal Topology by Ligand Functionalization: Functionalized Hkust-1 Derivatives. *Cryst. Growth Des.* **2014**, *14*, 6122−6128.
(76) Walton, K. S.; Sholl, D. S. Predicting Multicomponent Adsorption: 50 Years of the Ideal Adsorbed Solution Theory. *AIChE J.* **2015**, *61*, 2757−2762.
(77) Myers, A. L.; Prausnitz, J. M. Thermodynamics of Mixed-Gas Adsorption. *AIChE J.* **1965**, *11*, 121−126.

DOI: 10.1021/acs.jpcc.6b07493
J. Phys. Chem. C 2016, 120, 23044−23054